Estimation Enhancement by Trajectory Modulation for Homing Missiles

J.L. Speyer,* D.G. Hull,* and C.Y. Tseng†,
University of Texas, Austin, Texas
and
S.W. Larson‡
United States Air Force, Eglin AFB, Florida

For bearing-only measurements used in the guidance of homing missiles, guidance laws based upon the separation of estimation and guidance do not seem to be adequate. To enhance observability, the trajectory of a bank-to-turn missile is modulated by minimizing the trace of the Fisher information matrix. The calculations for constructing this performance index are greatly reduced by noting that the required transition matrix can be obtained in closed form because, in a relative rectangular coordinate system, the missile-target engagement dynamics are linear. To show significant improvement in estimation performance, the extended Kalman estimator is tested along both the enhanced observability trajectory and a proportional navigation trajectory. A Monte Carlo analysis is performed showing that, even for large initial estimation errors in range, range-rate, and target acceleration, convergence for the enhanced observability trajectory occurred within the homing period, whereas no convergence occurred for the proportional navigation path.

Nomenclature

A	= acceleration, ft/s^2
a,b	= constants in power spectral density relation
F,G,Γ	= constants in general dynamics equation
H	= matrix of partial derivatives, h_x
h	= measurement function
I_n	= $n \times n$ identity matrix
Q	= process noise power spectral density
R	= range, ft
t	= time, s
tr	= trace
U,V,W	= velocity components, ft/s
U,u	= control vector
V	= measurement noise power spectral density
v	= measurement noise
W	= weighting matrix
w	= process noise
X,Y,Z	= position components, ft
X,x	= state vector
z	= measurement vector
λ	= target maneuver reciprocal time constant, s^{-1}
Φ	= transition matrix

Subscripts

az	= azimuth
el	= elevation
M	= missile
T	= target
R	= relative

Introduction

WITH the development of the microprocessor, sophisticated guidance algorithms are becoming practical to implement. A great deal of attention has been given to guidance algorithms based upon some criterion of optimality as minimization of time or quadratic forms.[1] These guidance algorithms have been based upon the assumption that the full state space of the missile-target engagement is available and that filter performance is not influenced by the guidance law. If bearing-only measurements are available, the quality of the estimation of the state space depends upon the intercept trajectory, which is reflected by the system observability. For example, proportional navigation attempts to null the line-of-sight rate so that range and range-rate are not observable. Whereas the deterministic guidance laws for homing missiles do not include any aspect of the estimation problem, stochastic controllers (called dual controllers) explicitly account for filter performance but are quite complex to mechanize since they usually require the calculation of some form of the projected error variance.[2,3] Our current research objective is to develop a performance criterion which will reflect relative filter observability and also be compatible with current homing guidance law development.

The derivation of the performance criterion relies heavily on the formulation of the missile-target engagement scenario. First, the performance index is based upon the trace of the Fisher information matrix.[4,5] The trace is used because the integration associated with the information matrix commutes with the trace operation. Second, it is observed that the desired transition matrix required for the calculation of the information matrix is that associated with the dynamics assumed for the extended Kalman filter (EKF). Since the missile acceleration is measured with onboard accelerometers, the filter dynamics, which model the missile-target engagement, are linear, and the corresponding transition matrix is determined in closed form. Finally, the weighting elements used in the information matrix reflect the power spectral density of the passive sensor. The above three steps determine a scalar information performance criterion in a rather simple and elegant form.

In determining the maximum information trajectory, the information performance criterion is minimized with respect to the controls of yaw and pitch angle and subject to the equations of motion of a point mass representing a bank-to-turn missile. These equations of motion are quite nonlinear since the missile acceleration is modeled using a lift-drag polar which is a function of Mach number and angle of attack. Note that in the determination of the maximum information

Submitted April 30, 1982; revision received May 19, 1983.

*Professor, Department of Aerospace Engineering and Engineering Mechanics. Associate Fellow AIAA.
†Graduate Research Assistant, Department of Aerospace Engineering and Engineering Mechanics.
‡Captain. Associate Fellow AIAA.

trajectory detailed aerodynamic acceleration modeling is required, whereas acceleration is a measured input to the filter. Additional constraints included in the optimization formulation are the prescribed terminal constraints of zero miss and in-flight inequality constraints on angle of attack, normal acceleration, and boresight angle. For an initial aspect angle and boresight angle, an approximate optimal trajectory is calculated. The trajectory behavior is found to be somewhat oscillatory, varying the azimuth and elevation angles simultaneously.

The performance of the EKF is evaluated on this maximum information trajectory. The acceleration along the trajectory is made available to the filter; thus the guidance aspects of the problem are eliminated. The angle measurements are formed from the trajectory state and corrupted by additive noise. The performance of the EKF along the optimal information trajectory is compared with the performance of the EKF along a path generated by a proportional navigation guidance law. Along the maximum information trajectory dramatic improvement in the estimation of the state space, as measured by the Euclidean norm of the position, velocity, and acceleration estimation errors, is observed.

Information Performance Criterion

In this section, a scalar performance index representing the information content of a sequence of measurements is developed. First the information performance criterion is defined. Then the explicit form of the transition matrix, the measurement-function derivatives, and the measurement noise power spectral density, which reduce the information performance criterion without any additional approximation to a rather simple and elegant form, are presented.

Definition of a Scalar Information Performance Criterion

In selecting the performance index for enhancing filter performance, there are two main considerations. First, the performance index should represent the information content of a sequence of measurements. Second, classical optimization theory requires that the performance index be a scalar quantity.

A commonly used measure of accuracy in determining unknown parameters from a sequence of measurements is the Fisher information matrix.[4] Furthermore, it is shown in Ref. 5 that this matrix is an approximation of the curvature at the mode of the log-likelihood function associated with the sequence of measurements.

The Fisher information matrix can be related to the missile intercept problem through the local observability matrix when no process noise is considered and the additive measurement noise is white and Gaussian. This is because the estimation problem for the missile is represented in Cartesian coordinates as having linear dynamics and nonlinear measurements. Note that for this case the inverse of the error covariance of the linearized filter about a given nominal is the local observability matrix and also the Fisher information matrix.

The local observability matrix is given by

$$I(t_f,t_0)=\int_{t_0}^{t_f}\Phi^T(\tau,t_f)H^T(\bar{x}(\tau))V^{-1}(\bar{x}(\tau))\times H(\bar{x}(\tau))\Phi(\tau,t_f)\,d\tau \tag{1}$$

where $\bar{x}(\tau)$ represents the nominal path about which all linearizations are made. Also, $\Phi(\tau,t)$ is the inverse of the state transition matrix associated with the linearized dynamical equations used in the filter, and H is the partial derivative of the measurement function with respect to the state which results in the linearization of the measurement equation. Note that the transition matrix used in the filter is known in closed form suggesting an enormous reduction in the calculation of $I(t_f,t_0)$ over that of the general nonlinear problem. Finally, V is a weighting matrix taken to be the power spectral density of the measurement noise. It is normally evaluated along the estimate but is assumed here to be evaluated on the nominal.

In some sense, the size of a matrix can be measured by the sizes of its eigenvalues—the bigger the eigenvalues, the bigger the matrix. Two scalar operations on a matrix which relate to the eigenvalues are the trace and the determinant. The linear trace operation, which is the sum of the diagonal elements of the matrix, is also the sum of the eigenvalues. On the other hand, the nonlinear determinant operation forms the product of the eigenvalues. While the determinant is probably the better overall measure of the sizes of the eigenvalues, it requires much more computer time and storage to implement.[6] Furthermore, since only the trace commutes with the integral, a scalar integrand consistent with the forms of the performance index in the Bolza problem of the calculus of variations can be constructed. Hence, only the trace of the observability matrix is used as the performance criterion.

As will be shown later, the observability matrix is a 9×9 matrix associated with three relative position, three relative velocity, and three target acceleration estimates. Since the eigenvalues associated with these groups of estimates may be of considerably different magnitudes, the observability matrix is premultiplied by a constant weighting matrix W before the trace is formed. Then, since the trace and integration operations commute, the scalar information performance criterion is finally given by

$$J=\int_{t_0}^{t_f}\operatorname{tr}W\Phi^T(\tau,t_f)H^T(\bar{x}(\tau))V^{-1}(\bar{x}(\tau))H(\bar{x}(\tau))\Phi(\tau,t_f)\,d\tau \tag{2}$$

Physical Model Used by the Filter

The physical model assumed for the development of the filter is expressed in Cartesian inertial coordinates. The dynamical equations consist of the kinematic equations for relative position and relative velocity expressed as

$$\begin{aligned}\dot{X}_R&=U_R, & \dot{U}_R&=A_{T_X}-A_{M_X}\\ \dot{Y}_R&=V_R, & \dot{V}_R&=A_{T_Y}-A_{M_Y}\\ \dot{Z}_R&=W_R, & \dot{W}_R&=A_{T_Z}-A_{M_Z}\end{aligned} \tag{3}$$

Since missile acceleration is measured onboard, a model for target acceleration is required. Although it is preferred to model target acceleration as a Poisson process with given acceleration but random jump times, only diffusion processes can be included in the filter formulation. Therefore, the Poisson process is approximated by a first-order Gauss-Markov process with an identical autocorrelation. Hence, the dynamical equations for the target acceleration are given by

$$\dot{A}_{T_X}=-\lambda A_{T_X}+w_x,\quad \dot{A}_{T_Y}=-\lambda A_{T_Y}+w_Y$$
$$\dot{A}_{T_Z}=-\lambda A_{T_Z}+w_Z \tag{4}$$

where λ is the target maneuver time constant and $w\triangleq[w_X w_Y w_Z]^T$ denotes zero-mean white noise of power spectral density Q.

In terms of the 9×1 state vector

$$X=[X_R Y_R Z_R U_R V_R W_R A_{T_X} A_{T_Y} A_{T_Z}]^T \tag{5}$$

the dynamical equations can be written in the form

$$\dot{X}=FX+GU+\Gamma w \tag{6}$$

$$F=\begin{bmatrix}0 & I_3 & 0\\ 0 & 0 & I_3\\ 0 & 0 & -\lambda I_3\end{bmatrix},\quad G=\begin{bmatrix}0\\ -I_3\\ 0\end{bmatrix},\quad \Gamma=\begin{bmatrix}0\\ 0\\ I_3\end{bmatrix} \tag{7}$$

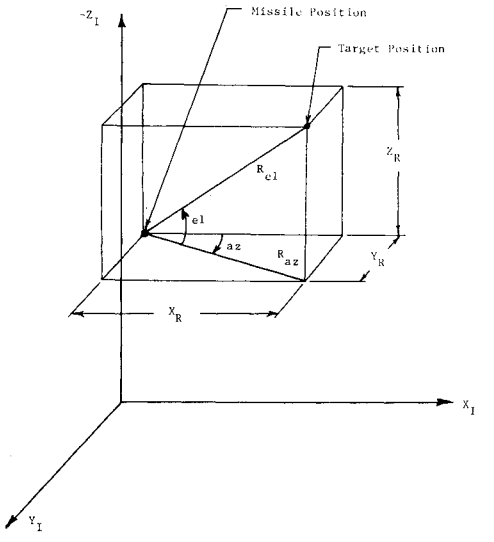

Fig. 1 Intercept geometry and measurement angles.

Also, the control $U=[A_{MX}A_{MY}A_{MZ}]^T$ is the 3×1 missile acceleration vector, $w=[w_X w_Y w_Z]^T$ is the noise associated with the target model, and I_n is an $n\times n$ identity matrix.

The measurements are the azimuth and the elevation of the target relative to the missile (Fig. 1) so that the measurement equations are given by

$$z_1=\tan^{-1}(Y_R/X_R)+v_1$$
$$z_2=\tan^{-1}(-Z_R/[X_R^2+Y_R^2]^{1/2})+v_2 \tag{8}$$

or in vector form by

$$z=h(X)+v \tag{9}$$

The quantity z denotes the measurement vector; h is the nonlinear measurement vector function; and v is a vector zero-mean white noise process with power spectral density V. The explicit form assumed for V is given in Eq. (17).

Linearization about the Normal

Given a nominal path $\bar{x}(t)$ and the corresponding control $\bar{u}(t)$, the actual state X and control U can be expressed as

$$X=\bar{x}+x, \qquad U=\bar{u}+u \tag{10}$$

where x and u are the state and control perturbations. If Eqs. (10) are substituted into Eq. (6), the state equation becomes

$$\dot{x}=Fx+Gu+w-(\dot{\bar{x}}-F\bar{x}-G\bar{u}) \tag{11}$$

It is important to recognize that the missile is assumed instrumented with accurate accelerometers to measure inertial forces. By using these acceleration values, the dynamics used by the onboard filter are linear. However, in calculating the nominal state, the control variables are aerodynamic angles on which the accelerations depend in a nonlinear way. In conclusion, the nominal inertial acceleration $\bar{u}$ of the missile and the zero-mean acceleration of the target cause the term in parentheses in Eq. (11) to vanish so that the dynamical equation for the perturbed state remains

$$\dot{x}=Fw+Gu+w \tag{12}$$

The linearization of the measurement equation leads to

$$z=h(\bar{x})+H(\bar{x})x+v \tag{13}$$

where H is the 2×9 matrix of partial derivatives of h with respect to the state. The nonzero elements of H are given by

$$H_{11}=h_{1x_1}=Y_R/R_{az}^2, \qquad H_{12}=h_{1x_2}=X_R/R_{az}^2$$
$$H_{21}=h_{2x11}=X_R Z_R/(R_{el}^2 R_{az}), \qquad H_{22}=h_{2x_2}=Y_R Z_R/(R_{el}^2 R_{az})$$
$$H_{23}=h_{2x_3}=-R_{az}/R_{el}^2 \tag{14}$$

where, as shown in Fig. 1,

$$R_{az}=(X_R^2+Y_R^2)^{1/2}, \qquad R_{el}=(X_R^2+Y_R^2+Z_R^2)^{1/2} \tag{15}$$

State Transition Matrix

In addition to the derivatives of the measurement function, the evaluation of the observability matrix requires the state transition matrix associated with Eq. (12). Because of the simplicity of the matrix F, the state transition matrix has been derived in closed form. The nonzero elements of $\Phi(t,\tau)$ are given as

$$\Phi_{11}=\Phi_{22}=\Phi_{33}=\Phi_{44}=\Phi_{55}=\Phi_{66}=1$$
$$\Phi_{14}=\Phi_{25}=\Phi_{36}=\Delta t,\ \Phi_{77}=\Phi_{88}=\Phi_{99}=\exp(-\lambda\Delta t)$$
$$\Phi_{47}=\Phi_{58}=\Phi_{69}=-(1/\lambda)[\exp(-\lambda\Delta t)-1]$$
$$\Phi_{17}=\Phi_{28}=\Phi_{39}=(1/\lambda^2)[\exp(-\lambda\Delta t)+\lambda\Delta t-1] \tag{16}$$

where $\Delta t\triangleq t-\tau$. To obtain the matrix $\Phi(\tau,t)$ needed by the observability matrix, the identity $\Phi(\tau,t)=\Phi^{-1}(t,\tau)$ can be employed. The nonzero elements of this matrix are given by Eq. (16) with Δt replaced by $-\Delta t=\tau-t$.

Power Spectral Density

The 2×2 diagonal matrix V represents the power spectral density of the angle measurement noise. Its elements are assumed to be

$$V_{11}=a/R_{az}^2+b, \qquad V_{22}=a/R_{el}^2+b \tag{17}$$

where V_{11} is associated with azimuth and V_{22} with elevation. The off-diagonal elements are zero. Normally, V is inversely related to the range. However, when the elevation approaches 90 deg, it is difficult to measure azimuth accurately. Hence, in V_{11}, the range has been replaced by R_{az} to account for this effect. The term a/R_{az}^2 represents uncertainty in target position (glint), while the constant b represents a fading-type noise. The values used here are

$$a=0.25\ \text{rad}^2\ \text{ft}^2\ \text{s}, \quad b=56.25\times 10^{-8}\ \text{rad}^2\ \text{s} \tag{18}$$

Weighting Matrix

The constant 9×9, diagonal weighting matrix W is used to normalize the terms in the observability matrix due to relative position, relative velocity, and target acceleration. The values used here are given by

$$W_{11}=W_{22}=W_{33}\triangleq W_1=1, \qquad W_{44}=W_{55}=W_{66}\triangleq W_2=t_f^{-2}$$
$$W_{77}=W_{88}=W_{99}\triangleq W_3=e^{-2tf} \tag{19}$$

Had these weights not been introduced, the target acceleration terms would have dominated the other terms as explicitly shown in Eq. (20).

Simplified Form of Information Performance Criterion

If Eq. (2) is combined with the expressions for H, Φ, V, and W, the following simplified and elegant form of the in-

Table 1 Intercept results

Trajectory	Flight time T_f, s	Performance index	Miss distance, ft X_R	Y_R	Z_R
Maximum information	5.84	16.2	0.011	0.039	0.002
Proportional navigation	2.66	4.94	0.026	−0.171	−0.218

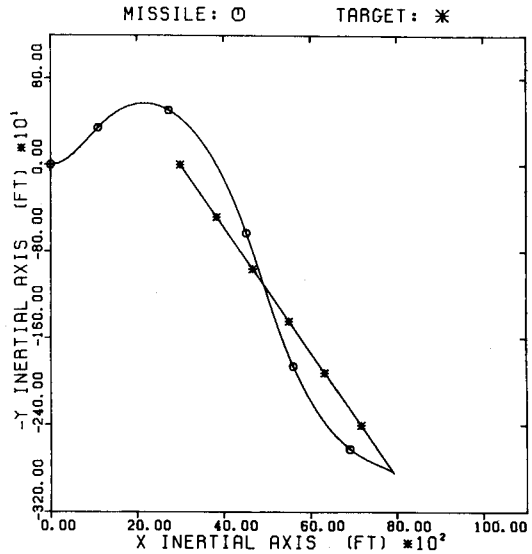

Fig. 2 Maximum-information trajectory, horizontal projection.

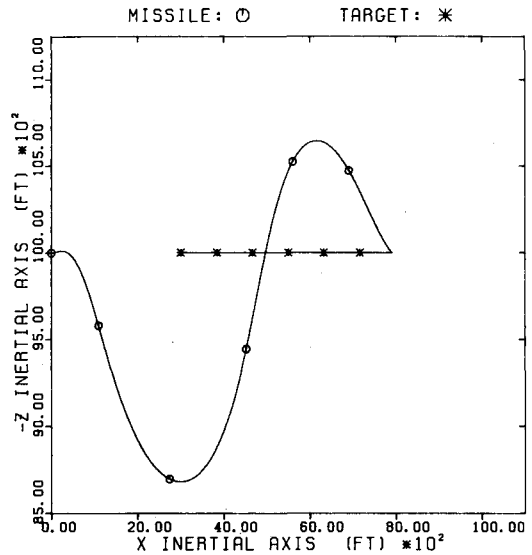

Fig. 3 Maximum-information trajectory, vertical projection.

formation performance criterion can be obtained:

$$J=\int_{t_0}^{t_f}\left[(a+bR_{az}^2)^{-1}+(a+bR_{el}^2)^{-1}\right]\left[W_1\Phi_{11}^2+W_2\Phi_{14}^2+W_3\Phi_{17}^2\right]d\tau \tag{20}$$

Note that the integrand is the product of a term containing relative position components and a term which contains only t and t_f.

Physical Model Used for Optimization

To complete the formulation of the optimization problem, it is necessary to discuss the modeling of the missile and the target, the boundary conditions, and the inequality constraints.

Since missile time constants are usually between 0.1 and 0.3 s and since the flight times are considerably larger than the time constants (see Table 1), the effect of small lags on the trajectory should be negligible. Hence, the bank-to-turn missile is modeled as a point mass so that its motion is governed by a set of nonlinear differential equations. These equations are the three kinematic equations giving the inertial position of the missile center of gravity and the three dynamic equations giving the magnitude and direction of the missile velocity vector. The Earth is assumed to be flat with a constant acceleration of gravity and a standard atmosphere. The thrust has a constant magnitude for 2.6 s, and the mass flow rate is assumed constant so that the mass is a known function of time. The aerodynamics are typical of a theoretical bank-to-turn missile and are presented in tabular form as functions of Mach number and angle of attack. These tables are read by linear interpolation. Finally, the control variables are chosen to be the yaw and pitch angles of the body centerline.

The target is assumed to have zero acceleration. Hence, it is traveling in a straight line at constant speed.

The initial conditions are those for a co-altitude, co-speed launch with a given range to the target. Also, the target off-boresight angle is assumed to be zero, and the aspect angle has been taken to be 30 deg. The prescribed final conditions are that the final relative positions be zero (zero terminal miss).

Several inequality constraints exist for this model. First, the angle of attack and the normal acceleration are limited. Second, in an attempt to model the seeker, the boresight angle (the angle between the line of sight to the target and the missile centerline) is limited to 60 deg.

The Optimization Problem

In general, the optimization problem is to maximize the information performance index subject to a set of differential constraints (equations of motion) with known initial conditions, a set of prescribed final conditions (zero terminal miss), and some control variable inequality constraints (on angle of attack, normal acceleration, and boresight angle). To simplify the problem, each inequality constraint is converted into a penalty-type constraint which, in turn, can be reduced to a differential constraint and an equality final condition.

At this point, the optimal control problem is reformulated as a nonlinear programming problem. This is accomplished in two steps. First, the time is normalized with respect to the final time, making t_f a parameter. Second, each control history is replaced by a set of nodal points and some form of interpolation. In this study, interpolation has been performed with cubic splines since a better approximation of the true optimal control can be achieved with fewer parameters.[7] The initial and final slopes are unknown so they are included as unknown parameters. In summary, the unknown p parameters are the final time, the nodal points of each control history, and the initial and final slopes of each control history. Once a set of these parameters is given, the differential equations can be integrated to obtain the final state as a function of the parameters. This means that the performance index and the final conditions can be considered as functions of the unknown parameters.

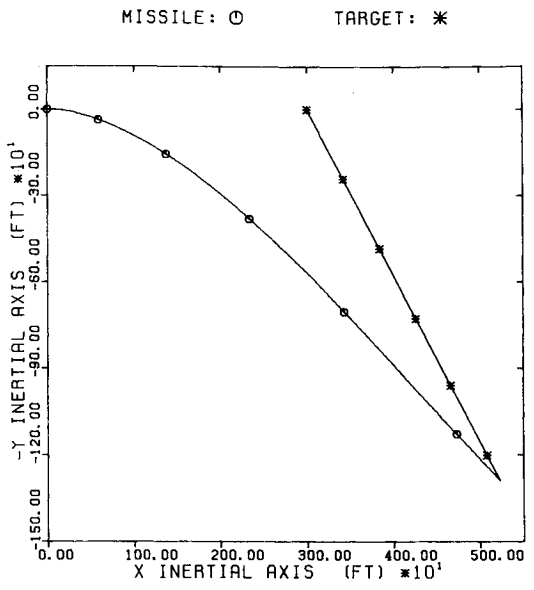

Fig. 4 Pro-nav trajectory, horizontal projection.

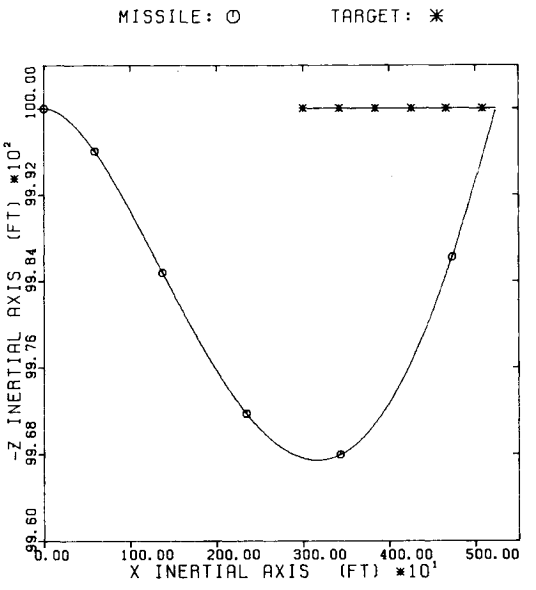

Fig. 5 Pro-nav trajectory, vertical projection.

Table 2 Initial state estimate statistics

State estimate element	Mean	Variance
$\hat{X}_R$	True value	10 ft^2
$\hat{Y}_R$	True value	10 ft^2
$\hat{Z}_R$	True value	10 ft^2
$\hat{U}_R$	True value	10 ft^2/s^2
$\hat{V}_R$	True value	10 ft^2/s^2
$\hat{W}_R$	True value	10 ft^2/s^2
$\hat{A}_{T_X}$	0 ft/s^2	2.5×10^4 ft^2/s^4
$\hat{A}_{T_Y}$	0 ft/s^2	2.5×10^4 ft^2/s^4
$\hat{A}_{T_Z}$	0 ft/s^2	2.5×10^4 ft^2/s^4

In view of the above discussion, the form of the nonlinear programming problem considered here is the following: Find the p vector y of parameters which minimizes the performance index $J=F(y)$ subject to the m vector of equality constraints $C(y)=0$. A maximization problem is converted into a minimization problem by multiplying the performance index by a minus sign.

Maximum-Information Trajectory

The particular method which has been chosen to solve the optimization problem is known as the augmented-Lagrangian method.[8] It is a penalty function method which allows convergence to be achieved without having to drive the weights to infinity. The particular code used has been obtained from the Atomic Energy Research Establishment in Harwell, England. Derivatives needed to perform the optimization are computed numerically by central differences.

The co-altitude, co-speed launch occurs at 10,000 ft and 0.9 Mach while the range is 3000 ft. As stated previously, the off-boresight angle is 0 deg, and the aspect angle is 30 deg. Each control history has been represented by five parameters: three nodes and two slopes. The results are summarized in Table 1. Also presented in Table 1 for comparison are the characteristics of the trajectory using proportional navigation guidance which is essentially a minimum-time path. It is discussed in the next section.

The geometry of the maximum-information trajectory is shown in Figs. 2 and 3. It is seen that this trajectory tries to vary the azimuth and the elevation simultaneously. Furthermore, the initial part of the trajectory is a transient maneuver which puts the missile on the desired intercept path. The value of the performance index is shown in Table 1 along with that calculated along the pro-nav trajectory. It is interesting to note that the maximum information path requires almost twice as much flight time as the proportional navigation path. Obviously the extra time is being used to modulate the trajectory to improve its information content.

Of all the inequality constraints, only the boresight angle constraint is ever in effect. Also of concern but not included as a constraint is the boresight angle rate. Fortunately, the maximum boresight angle rate encountered along the maximum information path is around 54 deg/s. This value can be achieved with current seekers.

Proportional-Navigation Trajectory

The pro-nav trajectory is obtained by the continuous use of the guidance law obtained from the linear-quadratic formulation discussed in Ref. 9. The state estimates required by this control law are taken to be the true relative position, relative velocity, and target acceleration. Also, the time-to-go required by the gains is computed as range over range-rate where range and range-rate are obtained from the true relative position and relative velocity.

This guidance law produces a commanded inertial acceleration which is transformed into the wind or velocity axes. Since it cannot be controlled, the acceleration component in the direction of the velocity vector is ignored. At this point, a perfect autopilot is assumed, and the acceleration component normal to the velocity vector is used to determine the bank angle and the angle of attack needed to produce the normal acceleration. This is accomplished by rolling the missile until the lift vector is aligned with the commanded normal acceleration vector. Then the angle of attack which makes the lift divided by the mass equal in magnitude to the normal acceleration is determined. Finally, the angle of attack and bank angle are input to the three-degree-of-freedom model of the missile which, when integrated, yields the motion of the missile.

The previous results have been obtained for the case where the process noise in the filter model is zero. Since process noise is present in the assumed model for the target acceleration, some filter results were obtained for two levels of process noise, that is, process noise with a power spectral density of $Q=100$ ft^2/s^5 and that with $Q=10{,}000$ ft^2/s^5. Also, the results are for the case of better measurements ($\sigma_2=10^{-1}\sigma_1$) and $\hat{X}_R=X_R+500$ ft at $t=0$. For $Q=100$ ft^2/s^5 the max-info trajectory enables the filter to reduce the

range error to a level around 100 ft, while the filter diverges for the pro-nav path. For $Q = 10{,}000$ ft^2 s^5 (Fig. 12), the filter diverges along the pro-nav path, and after two attempts to converge, it also diverges along the max-info path. In general, the filter tracks better along the max-info path than it does along the pro-nav path.

In the range error and range-rate error results of Figs. 6-12 for the max-info path, there is a rapid decrease in the error in the neighborhood of $t/t_f = 0.5$. It is speculated that this occurs because the line-of-sight rate is a maximum near this time (see Figs. 2 and 3) which enhances the observability of the state space.

Actually, the commanded inertial acceleration should have been projected onto the body axes instead of the wind axes. However, it is assumed that the angle of attack is small so that wind axes are approximate body axes. For the trajectory calculated with the above procedures, the angle of attack is less than 10 deg over the entire path.

The horizontal and vertical projections of the pro-nav trajectory are shown in Figs. 4 and 5. The terminal portion of the trajectory has the appearance of a classical intercept path (straight line). The initial part of the path just turns the missile onto the intercept trajectory. Finally, there is a very slight dip in altitude during the flight.

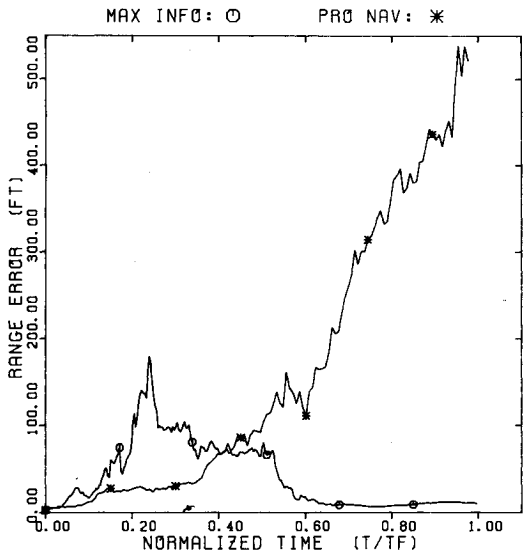

Fig. 6 Range error history.

Filter Performance

In this section, the performance of the extended Kalman filter along the maximum information (max-info) path is compared with that along the proportional-navigation (pro-nav) path. The intent is to show that, for filter problems with nonlinear dynamics and/or measurements, the performance of the filter should be a major consideration in the design of guidance laws.

For a given trajectory, measurements are created every 0.02 s, which is the filter sample time. This is done by adding to the true azimuth and elevation [see Eq. (8)] zero-mean white noise with noise variance $50(a/R^2 + b)$ where R is the true range and where a,b are defined in Eq. (18). By using a prescribed trajectory to form the noisy measurements, the performance of the filter is studied independently of the guidance law.

The physical model on which the filter is based has been presented in Eqs. (3)-(9). It is assumed that the measurements of missile acceleration are perfect. However, accelerometers can only measure aerodynamic accelerations (due to drag, lift, and thrust) so that the missile acceleration components in Eq. (3) are given by

$$A_{M_X} = \bar{A}_{M_X}, \quad A_{M_Y} = \bar{A}_{M_Y}, \quad A_{M_Z} = \bar{A}_{M_Z} + g \qquad (21)$$

where the bar denotes "aerodynamic" and $g = 32.2$ ft/s^2. The target maneuver time constant is chosen to be $\lambda = 1$. For the first part of this study, the process noise associated with the target model is assumed to be zero because the maximum information performance criterion is based on zero process noise. However, later in the study, filter performance will be evaluated with process noise present. Finally, the measurement noise variance is calculated where $R \triangleq \hat{R} = [\hat{X}_R^2 + \hat{Y}_R^2 + \hat{Z}_R^2]^{1/2}$ where the hat denotes estimates from the EKF.

The performance of the filter is measured in terms of tracking errors. These errors are the range error, the range-rate error, and the target acceleration error defined as follows:

$$\text{Range error} \equiv [(X_R - \hat{X}_R)^2 + (Y_R - \hat{Y}_R)^2 + (Z_R - \hat{Z}_R)^2]^{1/2}$$

$$\text{Range-rate error} \equiv [(U_R - \hat{U}_R)^2 + (V_R - \hat{V}_R)^2 + (W_R - \hat{W}_R)^2]^{1/2}$$

$$\text{Target acceleration error} \equiv [(A_{T_X} - \hat{A}_{T_X})^2 + (A_{T_Y} - \hat{A}_{T_Y})^2 + (A_{T_Z} - \hat{A}_{T_Z})^2]^{1/2} \qquad (22)$$

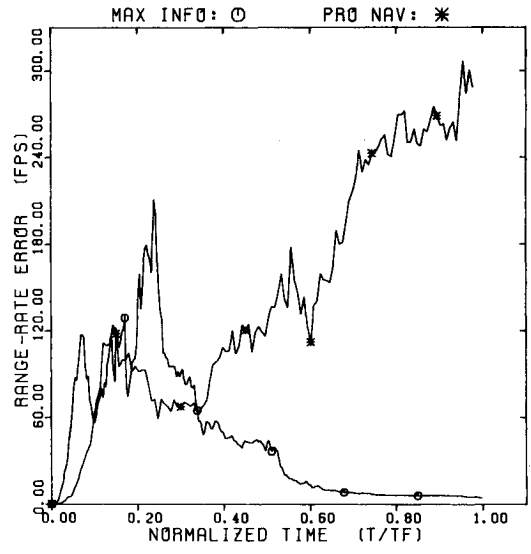

Fig. 7 Range-rate error history.

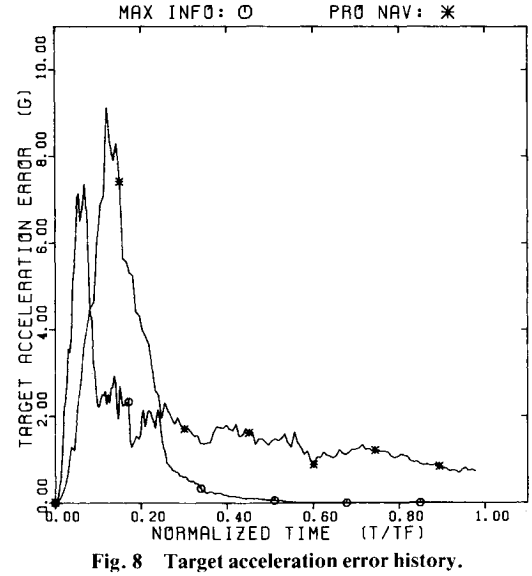

Fig. 8 Target acceleration error history.

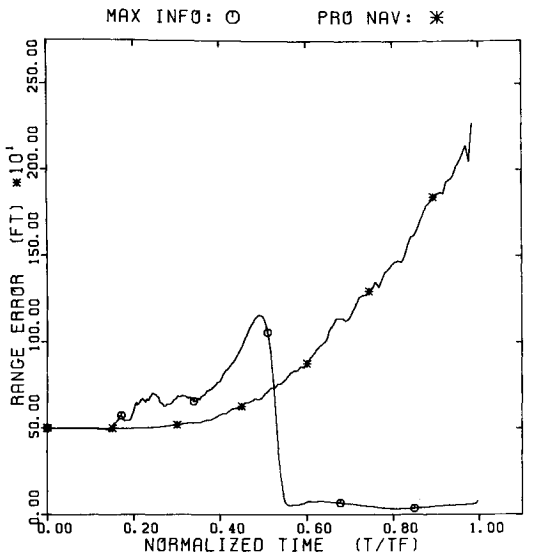

Fig. 9 Range error history, initial range error = +500 ft.

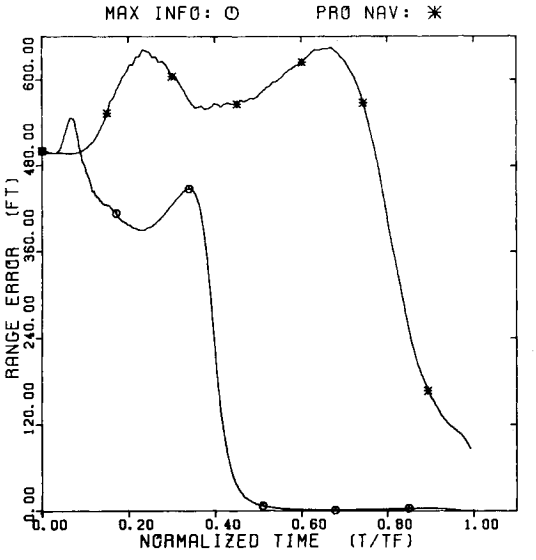

Fig. 11 Range error history, $\sigma_2 = 10^{-1}\,\sigma_1$.

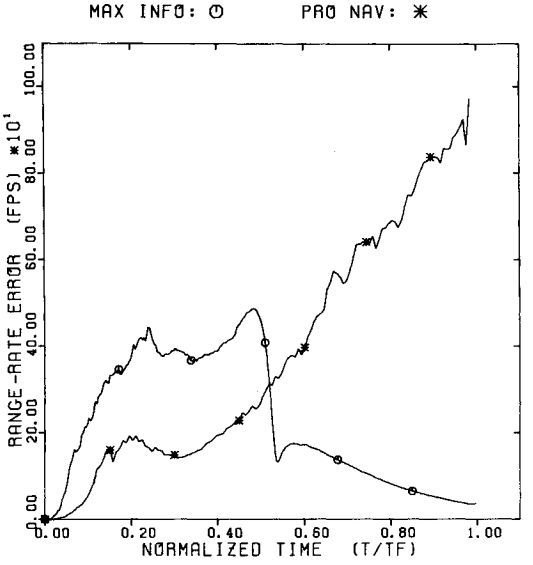

Fig. 10 Range-rate error history, initial range error = +500 ft.

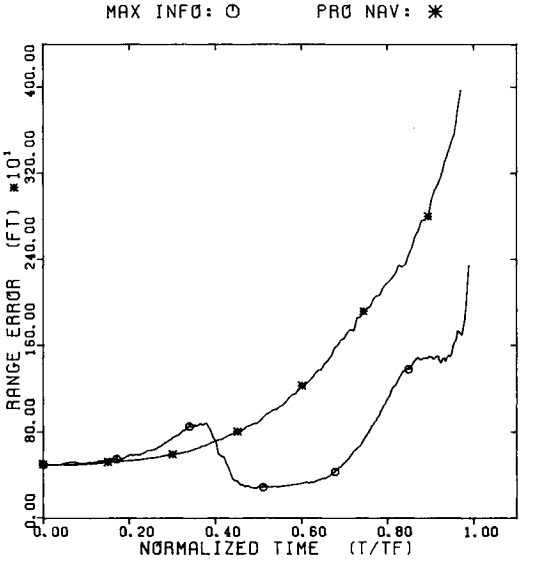

Fig. 12 Range error history, $Q = 10{,}000\ \text{ft}^2/\text{s}^5$.

The errors are plotted vs a normalized time, t/t_f, where t_f is the final time. All of the results presented here are the averages of 10 Monte Carlo runs. The runs are made, and the results of each sample time are averaged. To have a scale small enough to see the results, it has been necessary to eliminate the last three points from each curve. These points are not important because they are within times-to-go which are much smaller than the time constant of a typical autopilot and therefore would not have any effect on guidance accuracy.

For the first set of filter runs, the initial filter statistics are those presented in Table 2. The variances for the relative position and relative velocity are representative of measurements made with a good radar. The variances for the target acceleration components are based on a standard deviation of 5g. Figures 6-8 present the range, range-rate, and target acceleration tracking errors for the max-info path and the pro-nav path. It is seen that all three errors for the max-info path increase during the first one-third of the trajectory and then steadily go to zero over the last two-thirds of the path. For the pro-nav trajectory, the range and range-rate errors increase with time and show no sign of converging. On the other hand, the target acceleration error decreases with time, but it never goes to zero. Initially, the pro-nav path seems to lead to smaller tracking errors than the max-info path. However, if the errors are plotted vs time rather than normalized time, the initial error histories would be similar. In conclusion, the max-info path enables the filter to track the target, whereas the same is not true for the pro-nav path.

Figures 9 and 10 show the effect of a +500-ft error in the relative position component $\hat{X}_R$. The acceleration profile is similar to Fig. 8. The filter uses an initial range of 3500 ft instead of 3000 ft. The conclusions reached from these figures are the same as those for the figures with no errors. The max-info path enables the filter to converge to the true results, whereas the pro-nav path causes the filter to diverge on range and range-rate and converge to the wrong result in target acceleration. The results are the same when there are initial biases in velocity or acceleration.

In order to show the effect of improved measurements, the Monte Carlo runs have been made with a and b in the measurement covariance reduced two orders of magnitude. Written in terms of the standard deviation, this means that $\sigma_2 = 10^{-1}\sigma_1$, where σ_1 is the original standard deviation and σ_2 is the standard deviation of the improved measurements. The results for range error are presented in Fig. 11 for the case

where the initial value of $\hat{X}_R$ is 500 ft greater than the true value. The first observation from these figures is that the improved measurements allow the filter to converge along the pro-nav path, whereas before it diverged for the range. Second, with the exception of the target acceleration error, the maximum value of the tracking error for the max-info path is about one-half what it was for the original measurements. Finally, the max-info path enables the filter to converge sooner with better measurements than before.

The previous results have been obtained for the case where the process noise in the filter model is zero. Since process noise is present in the assumed model for the target acceleration, some filter results were obtained for two levels of process noise, that is, process noise with a power spectral density of $Q = 100$ ft^2/s^5 and that with $Q = 10{,}000$ ft^2/s^5.

Conclusions

An information performance criterion has been proposed for computing missile trajectories which enhances the ability of an onboard guidance filter to estimate the state. Noisy measurements are created along the max-info and pro-nav paths by adding zero-mean white noise to the true azimuth and elevation. These measurements are processed by an extended Kalman filter to determine the effect of the trajectory on the performance of the filter. Monte Carlo runs have been made for no process noise, a given measurement covariance, and no errors in the initial state estimates. Then, in sequence, errors have been introduced in the state estimates; the measurement covariance has been reduced; and process noise has been introduced. In all cases, the max-info path enables the filter to perform better than it does along the pro-nav path. In fact, the pro-nav path leads to filter divergence in most cases. This demonstrates clearly the need to develop homing missile guidance laws for passive seekers which are based partly upon estimation performance. The information performance criterion developed here is sufficiently simple so as to form the basis for guidance law development without the usual separation assumption. Variations of this criterion, such as the average information obtained by dividing by the flight time, might have additional advantages.

Finally, although the trajectory shown took approximately 1300 s of computation time on the UT Cyber 170/750, techniques and simplifications are being considered which may allow onboard computations.

Acknowledgment

This research was supported by the U.S. Air Force Armament Laboratory under Contract FO 8635-80-K-0350 managed by Capt. P.L. Vergez.

References

[1] Pastrick, H.L., Seltzer, S.M., and Warren, M.E., "Guidance Laws for Short-Range Tactical Missiles," *Journal of Guidance and Control*, Vol. 4, March-April 1981, pp. 98-108.

[2] Tse, E., Bar-Shalom, Y., and Meier, L., "Wide-Sense Adaptive Dual Control for Nonlinear Stochastic Systems," *IEEE Transactions on Automatic Control*, Vol. AC-18, April 1973, pp. 98-108.

[3] Tse, E. and Bar-Shalom, Y., "Adaptive Dual Control for Stochastic Nonlinear Systems with Free End-Time," *IEEE Transactions on Automatic Control*, Vol. AC-20, Oct. 1975, pp. 670-675.

[4] Mehra, R.K., "Optimal Input Signals for Parameter Estimation in Dynamic Systems—Survey and New Results," *IEEE Transactions on Automatic Control*, Vol. AC-19, No. 6, 1974, pp. 753-768.

[5] van der Waerden, B.L., *Mathematical Statistics*, Springer-Verlag, New York, 1969.

[6] Goodwin, G.C., Zarrop, M.B., and Payne, R.L., "Coupled Design of Test Signals, Sampling Intervals, and Filters for System Identification," *IEEE Transactions on Automatic Control*, Vol. AC-19, No. 6, 1974, pp. 748-752.

[7] Hull, D.G., and Williamson, W.E. Jr., "Nonlinear Method for Parameter Identification Applied to a Trajectory Estimation Problem," *Journal of Guidance and Control*, Vol. 1, July-Aug. 1978, pp. 286-288.

[8] Fletcher, R., "An Ideal Penalty Function for Constrained Optimization," *Journal of the Institute of Mathematics and Its Applications*, Vol. 15, 1975, pp. 319-342.

[9] Speyer, J.L., and Hull, D.G., "Comparison of Several Extended Kalman Filter Formulations for Homing Missile Guidance," *Proceedings of the AIAA Guidance and Control Conference*, Danvers, Mass., Aug. 1980, pp. 392-398.